Desalination and Water Treatment
www.deswater.com
doi: 10.1080/19443994.2014.907748

54 (2015) 3248–3256
June

Taylor & Francis
Taylor & Francis Group

Polypyrrole/polyaniline composites with enhanced performance for capacitive deionization

Yue Wang[a,b,c,*], Ruguo Wang[a,b], Shichang Xu[a,b,c], Qian Liu[a,b], Jixiao Wang[a,b,c]

[a]*Chemical Engineering Research Center, School of Chemical Engineering and Technology, Tianjin University, Tianjin 300072, P.R. China, Tel. +86 22 27404347; email: tdwy75@tju.edu.cn*
[b]*Tianjin Key Laboratory of Membrane Science and Desalination Technology, Tianjin 300072, P.R. China*
[c]*Synergetic Innovation Center of Chemical Science and Engineering, Tianjin 300072, P.R. China*

Received 23 September 2013; Accepted 19 March 2014

ABSTRACT

Polypyrrole/polyaniline (PPy/PANI) composites used for capacitive deionization were synthesized by *in situ* chemical oxidation polymerization method. The preparation parameters including the acid type, the acid concentration and the oxidant concentration were investigated and optimized in terms of the textual properties, the cyclic voltammetry tests, and the electrochemical impedance spectroscopy measurements. The obtained PPy/PANI composites present relatively uniform nanorod morphology with an average pore diameter of 13.1 nm. The specific capacitance of the composites under the optimal conditions is up to 341.4 F/g, which is approximately thrice that of pure PPy and twice that of pure PANI. The saturated adsorption capacity of the PPy/PANI–carbon nanotube (CNTs) cell was obtained as high as 197.8 mg NaCl/g, which is approximately 1.7 times of the PPy–CNT cell and 2.1 times of the PANI–CNT cell, respectively.

Keywords: Polypyrrole/polyaniline; Chemical oxidation polymerization; Capacitive deionization

1. Introduction

Recently, capacitive deionization (CDI) technology has evoked great attention due to its lower energy consumption and environmental friendly characteristics compared with the traditional technologies such as thermal and membrane desalination processes [1,2]. A typical CDI cell is technically assembled by two parallel electrodes, whose working principle can basically be described as the regular cycling of the adsorption process and the desorption process. During the adsorption process, a low direct current (DC) voltage is applied on the cell and the ions in the solution are adsorbed on the surface of the electrodes [3]. When the electrodes get to saturation, the cell voltage is then removed or reversed, at this stage the adsorbed ions are released back to the solution and the electrodes are regenerated [4,5]. By repeating the above steps, cyclic desalination of the CDI cell can be accomplished. Usually, for obtaining good performance of the CDI cell, a perfect electrode material is essential and significant [6,7].

Carbon materials, such as activated carbon fibers [8,9], hierarchical porous carbon [10], carbon nanotubes (CNTs) [11,12], and ordered mesoporous carbons [2], are commonly introduced to fabricate the

*Corresponding author.

CDI electrodes for their high specific surface area, porous structure, and good conductivity [13,14]. However, the ion adsorption behavior for carbon materials follows the double-layer principle and occurs only at the surface of the materials, which limits the further increase of the adsorption capacity and scaling-up application of the materials [15].

Metal oxides and conducting polymers belong to another type of electrode materials, which possesses pseudo-capacitance (also electrochemical capacitance). For this kind of material, the ions adsorption occurs not only on the surface, but also in the interior of the materials [15]. As a consequence, the specific capacitance of these materials is normally an order of magnitude higher than the carbon materials. However, considering the high cost of metal oxides and the possible contamination of the effluent induced by the heavy metals, only conducting polymers are more favorable materials for application in the CDI process.

Polypyrrole (PPy) and polyaniline (PANI) are two typical kinds of conducting polymers, which can realize their higher charge storage capacities by the n- and p-doping-undoping process of the polymer electrodes in a potential range [16]. Commonly, PANI exhibits higher capacitance and better mechanical strength than PPy as the references suggested [17-19], but these advantages can only be fully displayed under acidic environment, which restricts wide application of the material [20]. Referring to the PPy material, its electro-chemical properties are more stable for different pH environments. So it is believed that the combination of PPy and PANI can maximally explore the good properties of the two materials and simplify the polymerization procedures since both of them can be prepared by chemical oxidation polymerization method.

In this paper, the PPy/PANI composites were synthesized through *in situ* chemical oxidation polymerization method. The synthesis parameters, such as the acid type, the acid concentration, and the oxidant (ammonium persulfate, APS) concentration were investigated and optimized according to their textural properties and electrochemical properties. Desalination performance of the PPy/PANI composite electrode was also evaluated.

2. Experimental

2.1. Preparation of PPy/PANI composites

The PPy/PANI composites were prepared through *in situ* chemical oxidation polymerization method. The preparation was divided into two steps. One is for obtaining the dispersed PANI solution and the other for obtaining the PPy/PANI composite samples. For the first step, 0.05 g aniline was dispersed in the acid solution for 30 min, then the APS solution was dropped into the system and reacted for 1 h [21]. Finally, additional 0.228 g aniline was dosed and reacted for 4–6 h, and as a consequence the dispersed PANI solution was obtained. The above procedures were carried out in a 5℃ water bath suggested in the reference [22] and were accompanied with stirring all along.

For the second step, 0.278 g pyrrole (the mass ratio of pyrrole and aniline was fixed as 1:1) was dripped into the dispersed PANI solution and stirred for 20 min to make the pyrrole distribution even. Afterwards, $FeCl_3$ solution, used as oxidant for the polymerization of pyrrole, was added dropwise into the stirring system. The reaction concentration of $FeCl_3$ was fixed at 0.2 M according to our previous work on PPy/CNTs composites [23]; the polymerization time and temperature were referenced as 20 h and below 20℃, respectively [24,25]. After the polymerization, the reacting solution was filtered and the obtained PPy/PANI composite samples were washed with distilled water and dried at 60℃ under vacuum for 12 h.

2.2. Fabrication of experimental electrodes

The PPy/PANI composite electrode was fabricated by compression molding method. The PPy/PANI composites (as active component), polyvinylidene fluoride (PVDF, as binder), and graphite powder (as conductivity agent) were mixed at a weight ratio of 85:10:5 and ground adequately [26]. Then the well-mixed powders were put into the self-manufactured mold and pressed at a pressure of 10 MPa for about 5 min. After mold-releasing, the PPy/PANI plate with diameter of 15 mm and thickness of 2 mm was adhered on the disposed titanium plate to obtain the PPy/PANI electrode samples. Using the same method and conditions, the experimental PPy (obtained according to the second step of section 2.1) electrode, PANI (obtained in the first step of section 2.1) electrode, and CNTs (purchased from Chengdu Organic Chemicals Co. Ltd. Chinese Academy of Science, Muti-wall, diameter of 20–30 nm, length of 10–30 μm) electrode samples were fabricated and the corresponding three types of CDI cells (PPy/PANI-CNTs, PPy-CNTs, and PANI-CNTs) were assembled accordingly.

2.3. Description of the experimental CDI system

The desalination performance of the CDI cells was tested in an experimental system shown in Fig. 1.

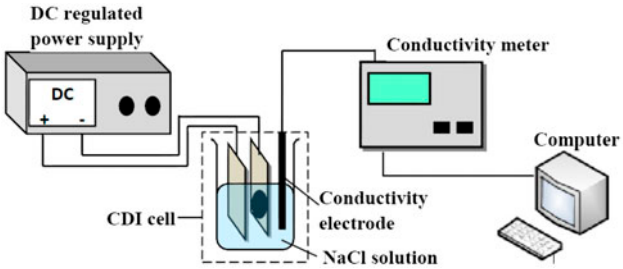

Fig. 1. Flow diagram of the CDI desalinating system.

Here, the working voltage of the CDI cells was provided by the DC-regulated power supply and fixed at 1.4 V. NaCl solution with a concentration of 500 mg/L was used as the experimental feed, whose conductivity was monitored and collected in real time accompanying the adsorption/desorption experiments of the CDI cells.

3. Results and discussion

3.1. Effects of acid type

Three types of acids including H_2SO_4 (1.5 M), HCl (1.5 M), and $HClO_4$ (1.5 M) were taken into account for the polymerization of PPy/PANI composites, especially for the prior synthesis of the dispersed PANI solution. Here, the concentration of the APS solution was fixed as 0.384 M.

The morphology of PPy/PANI composites was characterized using scanning electron microscopy (SEM). Typical images of PPy/PANI composites prepared in different acids are shown in Fig. 2. It is worthy of noting that the morphologies of the composites are diverse for different types of acids. For the H_2SO_4 acid, the PPy/PANI composites exist in the form of coral morphology, while for HCl and $HClO_4$ both the composites present nanorod morphology with slight agglomeration. Comparatively, the agglomeration phenomenon for PPy/PANI composites with HCl is more obvious than that with $HClO_4$, resulting in different textural properties of the composites shown in Table 1.

It can be seen from the table that the PPy/PANI product with the help of $HClO_4$ has the biggest BET specific surface area, BET specific mesoporous surface area and the highest pore volume. Besides, the ratio of BET specific mesoporous surface area to BET specific surface area reaches the maximum value of 87% (32.82/37.7) and the average pore diameter is 13.1 nm, which indicates that the composites are characterized with mesopore structure mainly. As reported, the big specific area might provide more points for adsorbing the ions and then can improve the material's adsorbing ability [27]. What more, the high pore volume and mesopores are of great benefit to enhance the diffusion of ions in the interior of the materials.

In order to evaluate the electrochemical properties of the PPy/PANI composite electrodes, cyclic voltammogram (CV) tests were carried out using a three-electrode system and in a 1.0 M KCl solution between −0.2 and 0.6 V vs. saturated calomel electrode (SCE) measured at a sweep rate of 5 mV·s^{-1}. Wherein, a platinum electrode and a SCE were used as a counter and a reference electrode, respectively. Fig. 3 shows the CV curves of the electrodes prepared in the presence of different acids. It can be seen that the current of PPy/PANI electrode prepared with the help of $HClO_4$ has a rapid change, which means there happens electrochemical reaction in the electrode and promises better doping consequence of the composites and good doping/de-doping rate of the electrode.

Calculated by formula (1) [28], the specific capacitance of PPy/PANI composite electrodes prepared in different acids is given in Table 2. From Table 2, the specific capacitance of the PPy/PANI composite with $HClO_4$ is much higher than that with HCl (7.5 times) and H_2SO_4 (116 times), though the BET-surface area of PPy/PANI composite with $HClO_4$ is slightly higher than that with HCl and with H_2SO_4 (see Table 1). This can be explained as follows: compared with Cl^-, the hydrated radius of ClO_4^- is smaller, promoting that it is easier to be doped for the composites. Concerning the SO_4^{2-}, its larger hydrated radius makes it more difficult to be doped compared to ClO_4^-. Moreover, in the presence of SO_4^{2-}, PPy tends to be cross-linked and carbonylated for β position C, which will damage the conjugated π-electron system of the backbone and thus prevent PPy from being doped. The poor doping consequence of PPy greatly decreases the specific capacitance of the PPy/PANI electrode with the help of H_2SO_4, though its BET surface area is slightly lower than that with $HClO_4$. Given that, $HClO_4$ is selected as the proper type of acid for preparation of PPy/PANI composites.

$$C = \frac{\frac{\int_{E_1}^{E_2} i(E)dE}{E_2 - E_1}}{mv} \tag{1}$$

where E_1 and E_2 are the initial and the final potential (V), respectively, i is the response current (A), v is the potential scan rate (V/s), and m is the mass of composite materials in the electrodes (g).

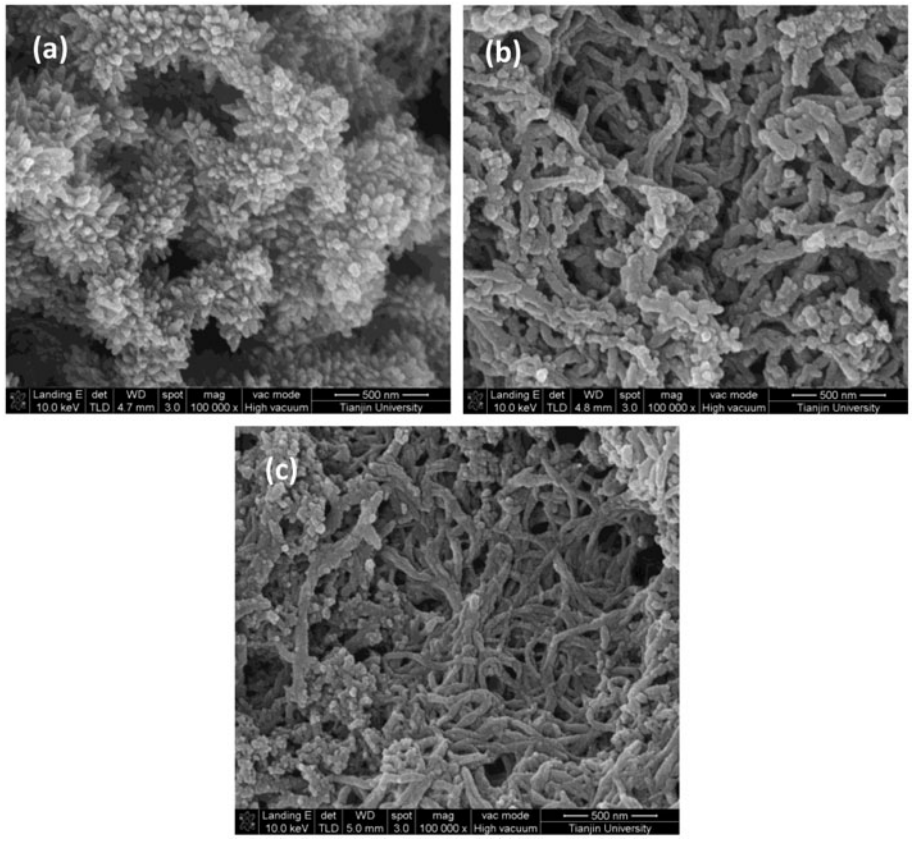

Fig. 2. SEM images of PPy/PANI composites prepared in the presence of H_2SO_4 (a), HCl (b) and $HClO_4$ (c).

Table 1
Textural properties of PPy/PANI composites prepared with different types of acid

Acid	S_{BET} (m^2/g)	S_{Meso} (m^2/g)	Pore V_{total} (cm^3/g)	Pore Dav (nm)
$HClO_4$	37.7	32.82	0.123	13.1
HCl	23.1	17.90	0.049	9.4
H_2SO_4	34.7	13.79	0.075	8.6

Notes: S_{BET}: BET specific surface area; S_{Meso}: BET specific mesoporous surface area; Pore V_{total}: pore volume of pores; Pore Dav: average pore diameter.

3.2. Effects of $HClO_4$ concentration

This section mainly investigated the effects of the $HClO_4$ concentration on the textural and electrochemical properties of the composites. Table 3 gives the textural properties of PPy/PANI composites prepared in different $HClO_4$ concentrations. Here, the remaining APS concentration is 0.384 M. It indicates that at $HClO_4$ concentration of 1.5 M, both the BET specific surface area and the pore volume of the composites reach their maximum (37.7 m^2/g and 0.123 cm^3/g, respectively), which does benefit for providing more points to adsorb the ions and enhancing the diffusion of ions in the interior of the electrode materials.

The CV curves of PPy/PANI composite electrodes prepared in different $HClO_4$ concentrations are showed in Fig. 4. It can be seen that weak redox peaks appear in the CV curves, illustrating the existence of the pseudo-capacitance for the electrode materials [29]. Table 4 presents the specific capacitance corresponding to the CV curves in Fig. 4. Therein, as $HClO_4$ concentration increases from 0.5 to 2.5 M, the specific capacitance of the electrodes increases initially

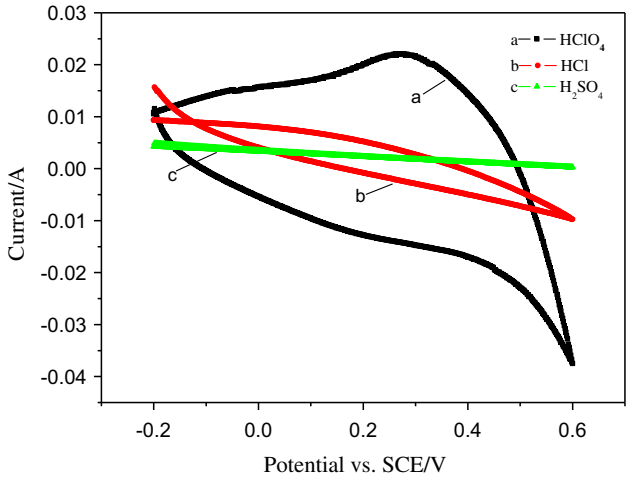

Fig. 3. CV curves of the PPy/PANI composite electrodes prepared in the presence of different acids.

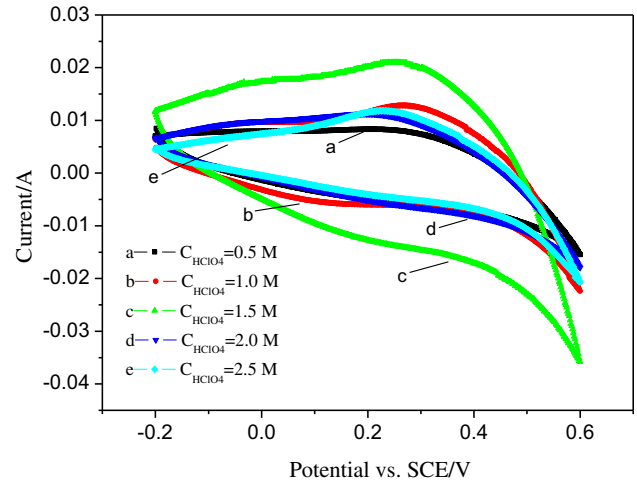

Fig. 4. CV curves of the PPy/PANI composite electrodes prepared with different $HClO_4$ concentration.

Table 2
Specific capacitance of PPy/PANI composites prepared with different types of acid

Acids	$HClO_4$	HCl	H_2SO_4
Specific capacitance (F/g)	139.2	18.5	1.2

Table 3
Textural properties of PPy/PANI composites prepared with different $HClO_4$ concentration

C_{HClO4} (M)	S_{BET} (m^2/g)	S_{Meso} (m^2/g)	Pore V_{total} (cm^3/g)	Pore Dav (nm)
0.500	35.0	32.47	0.099	11.3
1.000	32.2	29.97	0.096	11.9
1.500	37.7	32.82	0.123	13.1
2.000	31.7	27.10	0.080	10.1
2.500	23.1	17.90	0.054	9.4

and then declines, getting to the maximum at 1.5 M within the studied ranges.

As is known, $HClO_4$ provides not only the protons but also the dopants (ClO_4^-) necessary for the polymerization of aniline. So with the increase of the $HClO_4$ concentration, the doping level of the composites adds accordingly, which results in improved conductivity of the PPy/PANI composite. However, the side reactions will simultaneously be enhanced as the $HClO_4$ concentration increases, resulting in the reduction of overall specific capacitance of the composite [30]. So the maximum capacitance property obtained at $HClO_4$ concentration of 1.5 M is actually the coordinated effects of the added doping level and the reduced side reactions.

In order to investigate the effects of $HClO_4$ concentration on electrochemical resistance and the resistance of ion diffusion in the interior of the PPy/PANI composite electrode, the EIS (Electrochemical Impedance Spectroscopy) tests were carried out using the same three-electrode system as the CV tests in 1.0 M KCl solution with the frequency of 100 kHz to 10 mHz. The Nyquist plots of the composite electrodes prepared in different $HClO_4$ concentrations are drawn in Fig. 5. Each plot consists of a semi-circular arc in the high-frequency region and an inclined line in the low-frequency region. The radius of the semi-circular arc reflects the electrochemical resistance (also described as pseudo-transfer resistance) induced by the electrochemical reaction of the electrodes. The slope of the inclined line gives the resistance of ion diffusion in the interior of the electrode materials (also called the Warburg resistance), which is associated with the internal structure of the electrode materials.

From the plots in Fig. 5, the radius of the semi-circular arcs is quite different at various $HClO_4$ concentrations and follows in the order of $c < d < b < a < e$ which indicates that the electrochemical resistance also follows the same order and gets to the minimum at condition c ($HClO_4$ concentration of 1.5 M). Moreover, for the $HClO_4$ concentration of 1.5 M, the slope of the corresponding inclined line reaches the biggest, meaning that the ion diffusion resistance in the electrode comes to the lowest at the concentration [15]. Considering the high-specific capacitance, better electrochemical behavior and the lower electrode resistance, $HClO_4$ concentration of 1.5 M is recognized to be the optimal experimental condition.

Table 4
Specific capacitance of the PPy/PANI composite electrodes prepared with different $HClO_4$ concentration

C_{HClO_4} (M)	0.500	1.000	1.500	2.000	2.500
Specific capacitance (F/g)	100.6	130.1	212.4	115.0	105.9

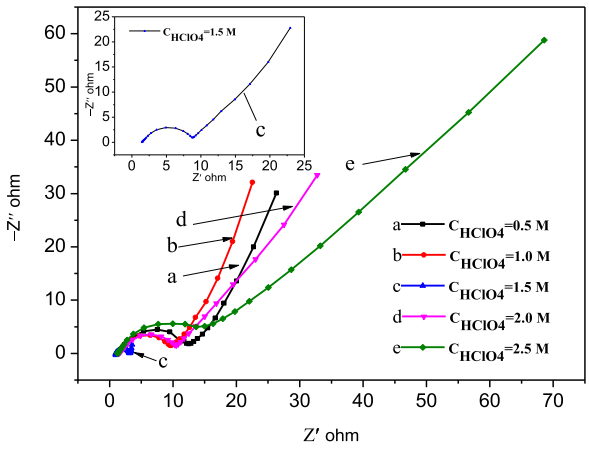

Fig. 5. The Nyquist plots of the PPy/PANI composite electrodes prepared with different $HClO_4$ concentration.

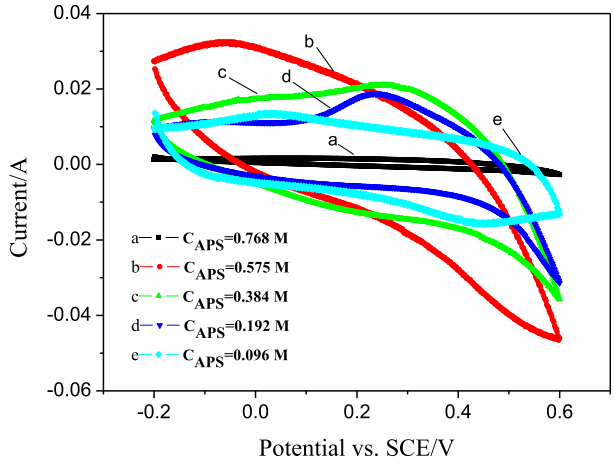

Fig. 6. CV curves of the PPy/PANI composite electrodes prepared with different APS concentration.

3.3. Effects of APS concentration

Fig. 6 illustrates the CV curves of PPy/PANI composite electrodes prepared at $HClO_4$ concentration of 1.5 M and APS concentration varying from 0.096 M to 0.768 M. It can be found that the obtained CV curves appear irregular at different APS concentrations. However, the calculated specific capacitance corresponding to the CV curves of the electrodes shown in Table 5 presents regular results. It indicates that the specific capacitance of the electrode rises gradually from 149.3 to 341.4 F/g as the APS concentration adds from 0.096 to 0.575 M, and it decreases sharply to 17.6 F/g when the APS concentration continually increases to 0.768 M.

The results can be explained as: for lower APS concentration, the active centers in the reaction system are sparse and it is liable to obtain longer PANI chain with long conjugated π-electron system and thus lower electrode resistance. However, for higher APS concentrations, the active centers become dense, the opportunity to form long PANI chain falls down significantly and the excess APS may do damage to the conjugated π-electron system of the backbone [30]. So the APS concentration of 0.575 M is believed to be the proper condition for the polymerization process.

Fig. 7 presents the Nyquist plots of the PPy/PANI composite electrode with the APS concentration changing from 0.096 to 0.768 M. As shown in the plots, the radius of the semi-circular arcs follows the sequence of D < E < B < A < C at different APS concentrations, meaning that lowest electrochemical resistance of the electrode lies at the APS concentration of 0.575 M (condition D). Besides, when the APS concentration is 0.575 M, the slope of the corresponding inclined line gets to the biggest which corresponds to the lowest ion diffusion resistance in the electrode. To summarize, the APS concentration of 0.575 M is considered as the optimal condition for the polymerization of the PPy/PANI composites.

So in this study, the optimal polymerization conditions for the PPy/PANI composites are 1.5 M $HClO_4$ solution (as the acid) and 0.575 M APS solution at fixed mass ratio of pyrrole and aniline (1:1) and $FeCl_3$ concentration of 0.2 M. The FTIR was used to confirm the polymerization of the PPy/PANI composites. The FTIR spectra of PPy/PANI composites prepared under the optimal polymerization conditions is shown in Fig. 8. The band at 1,576 cm^{-1} can be assigned to the stretching vibration of C=C in the quinonoid ring of PANI [31]. And the band at 1,298 cm^{-1} is the stretching vibrations of C–N of the secondary aromatic amine of PANI. Bands 1513 and 1,140 cm^{-1} are attributed to the skeleton vibration and the bending vibration of the ring of PPy [29]. The C–H stretching vibrations in the ring of PPy and C–H bending

Table 5
Specific capacitance of the PPy/PANI composite electrodes prepared for different APS concentrations

C_{APS} (M)	0.096	0.192	0.384	0.575	0.768
Specific capacitance (F/g)	149.3	164.7	212.4	341.4	17.6

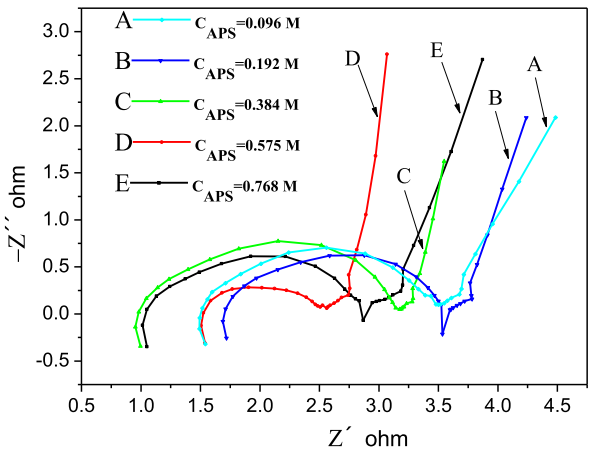

Fig. 7. The Nyquist plots of the PPy/PANI composite electrodes prepared at different APS concentration.

vibrations in the benzenoid ring of PANI appear at 2,890 and 800 cm^{-1}, respectively. The peak at 3,442 cm^{-1} is attributed to N–H stretching vibration of PPy. These bands of PPy and PANI indicate that PPy/PANI composites are successfully prepared.

Under the conditions, the specific capacitance of the obtained PPy/PANI composites was also tested and evaluated as high as 341.4 F/g, which is approximately triple of pure PPy (114.04 F/g) and twice of pure PANI (188.6 F/g). The superiority of the PPy/PANI composites may be attributed to co-effect of PPy and PANI. The high specific capacitance of PPy/PANI composites arises not only from good performance of PPy in neutral solution, but also from the fine electrochemical property of PANI which can be activated simultaneously when PPy is oxidized during the test.

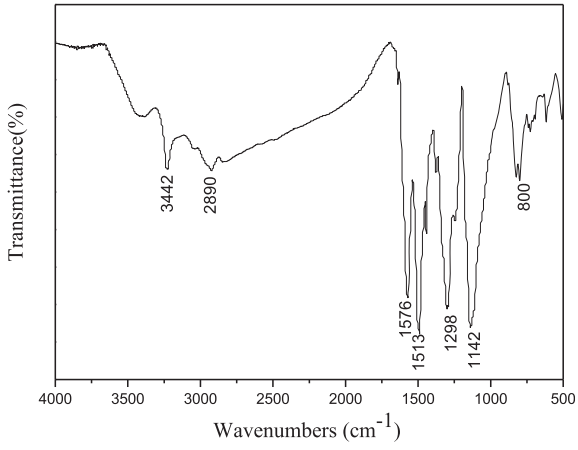

Fig. 8. FTIR spectra of PPy/PANI composites prepared under the optimal conditions.

3.4. Desalination tests

The desalination tests of the assembled CDI cells were carried out at a working voltage of 1.4 V in NaCl solution of 500 mg/L. Considering being doped with anion ions, the PPy/PANI composite electrode was specially used as the anode for fully displaying its pseudo-capacitance and an asymmetric-cell system was adopted to carry out the desalination tests using the CNTs electrode as the cathode. Fig. 9 gives the saturated adsorbing curves of PPy-CNTs, PANI-CNTs, and PPy/PANI-CNTs cells. It can be seen from the figure that the solution conductivity in the three curves shows the similar declining trend and the saturated adsorbing capacity of PPy/PANI-CNTs cell is obviously better than pure PPy and pure PANI. Through formula (2), the specific adsorption capacity of PPy/PANI-CNTs cell can be calculated as 197.8 mg NaCl/g, which is about 1.7 times of the PPy-CNTs cell (116.4 mg NaCl/g), 2.1 times of the PANI-CNTs cell (94.2 mg NaCl/g), and 3.7 times of the CNTs-CNTs cell (53.87 mg NaCl/g [23]).

$$m_t = \frac{(k_0 - k_1)\Lambda V}{m} \tag{2}$$

where m_t (mg NaCl/g) is the specific adsorption capacity of the cell to NaCl; k_0 and k_1 (μS/cm) are the initial and final conductivity of the solution, respectively; Λ is the coefficient between the conductivity and concentration of NaCl solution, and is measured as 6.48×10^{-3}; V (L) is the volume of the feed solution; and m (g) is the mass of the electroactive materials of the anode.

Additionally, cyclic performance of the PPy/PANI-CNTs cell was tested in 500 mg/L NaCl solution and the curve is shown in Fig. 10. Here, the adsorption time was set as 1,000 s considering the higher adsorption rate in the period (see Fig. 9), and desorption time

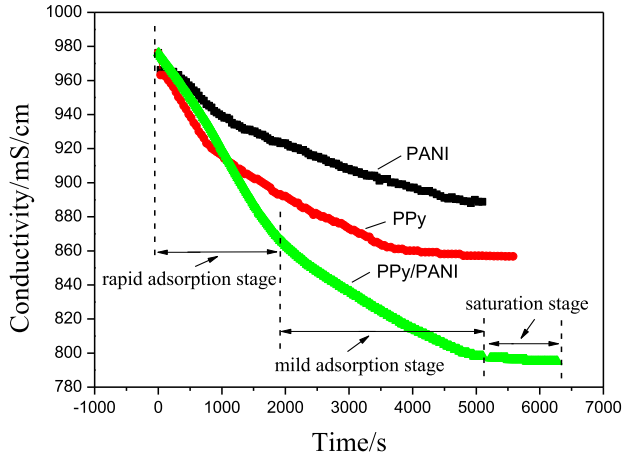

Fig. 9. Saturated adsorbing curve of PPy/PANI composite electrode working as anode at working voltage of 1.4 V in NaCl solution of 500 mg/L.

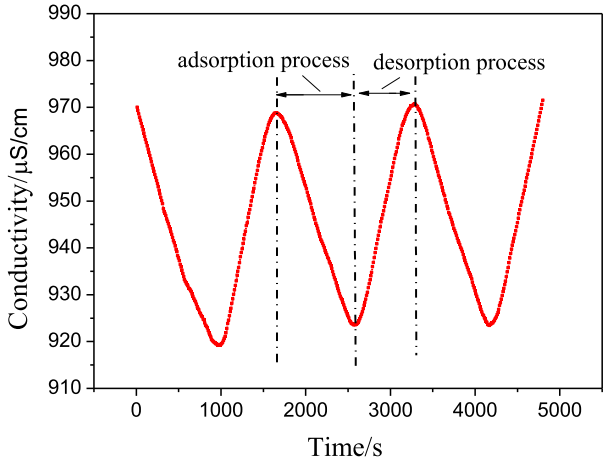

Fig. 10. Cyclic desalination performance of the PPy/PANI–CNTs cell in 500 mg/L NaCl solution at a working voltage of 1.4 V.

was fixed at 650 s experimentally. Fig. 10 indicates that the conductivity of the solution presents as "V" shape for the three experimental cycles and the conductivity of the solution can rebound to the initial value at the end of the desorption process, preliminarily manifesting the good adsorption and regeneration abilities of the PPy/PANI composite electrode.

4. Conclusions

(1) PPy/PANI composites for the capacitive deionization process were prepared through *in situ* chemical oxidation polymerization method. The preparation parameters are optimized and achieved as $HClO_4$ concentration of 1.5 M, APS concentration of 0.575 M under the fixed condition of 1:1 mass ratio of pyrrole, and aniline and $FeCl_3$ concentration of 0.2 M.

(2) The PPy/PANI composites present relatively uniform nanorod morphology with abundant mesopores. The composites have obvious superiority over pure PPy and pure PANI in the specific capacitance and the saturated adsorption capacity due to the co-effect of PPy and PANI.

(3) Further studies are needed in order to evaluate the composite cyclical stability after thousands of cycles and the performances in various salt solutions.

Acknowledgements

This research is supported by the National Natural Science Foundation of China [No.21276178].

References

[1] K.C. Leonard, J.R. Genthe, J.L. Sanfilippo, W.A. Zeltner, M.A. Anderson, Synthesis and characterization of asymmetric electrochemical capacitive deionization materials using nanoporous silicon dioxide and magnesium doped aluminum oxide, Electrochim. Acta 54 (2009) 5286–5291.

[2] Z. Peng, D. Zhang, L. Shi, T. Yan, High performance ordered mesoporous carbon/carbon nanotube composite electrodes for capacitive deionization, J. Mater. Chem. 22 (2012) 6603–6612.

[3] S. Porada, M. Bryjak, A. van der Wal, P.M. Biesheuvel, Effect of electrode thickness variation on operation of capacitive deionization, Electrochim. Acta 75 (2012) 148–156.

[4] S. Porada, L. Weinstein, R. Dash, A. van der Wal, M. Bryjak, Y. Gogotsi, P.M. Biesheuvel, Water desalination using capacitive deionization with microporous carbon electrodes, ACS Appl. Mater. Interfaces 4 (2012) 1194–1199.

[5] C. Nie, L. Pan, H. Li, T. Chen, T. Lu, Z. Sun, Electrophoretic deposition of carbon nanotubes film electrodes for capacitive deionization, J. Electroanal. Chem. 666 (2012) 85–88.

[6] F. Chen, P. Liu, Q. Zhao, Well-defined graphene/polyaniline flake composites for high performance supercapacitors, Electrochim. Acta 76 (2012) 62–68.

[7] L. Han, K.G. Karthikeyan, M.A. Anderson, J.J. Wouters, K.B. Gregory, Mechanistic insights into the use of oxide nanoparticles coated asymmetric electrodes for capacitive deionization, Electrochim. Acta 90 (2013) 573–581.

[8] Z.H. Huang, M. Wang, L. Wang, F. Kang, Relation between the charge efficiency of activated carbon fiber and its desalination performance, Langmuir 28 (2012) 5079–5084.

[9] G. Wang, C. Pan, L. Wang, Q. Dong, C. Yu, Z. Zhao, J. Qiu, Activated carbon nanofiber webs made by electrospinning for capacitive deionization, Electrochim. Acta 69 (2012) 65–70.
[10] J. Hu, H. Wang, X. Huang, Improved electrochemical performance of hierarchical porous carbon/polyaniline composites, Electrochim. Acta 74 (2012) 98–104.
[11] Y. Gao, L. Pan, H. Li, Y. Zhang, Z. Zhang, Y. Chen, Z. Sun, Electrosorption behavior of cations with carbon nanotubes and carbon nanofibres composite film electrodes, Thin Solid Films 517 (2009) 1616–1619.
[12] Y.X. Liu, D.X. Yuan, J.M. Yan, Q.L. Li, T. Ouyang, Electrochemical removal of chromium from aqueous solutions using electrodes of stainless steel nets coated with single wall carbon nanotubes, J. Hazard. Mater. 186 (2011) 473–480.
[13] M.A. Anderson, A.L. Cudero, J. Palma, Capacitive deionization as an electrochemical means of saving energy and delivering clean water. Comparison to present desalination practices: Will it compete? Electrochim. Acta 55 (2010) 3845–3856.
[14] Y. Zhang, Y. Wang, S. Xu, J. Wang, Z. Wang, S. Wang, Polypyrrole nanowire modified graphite (PPy/G) electrode used in capacitive deionization, Synth. Met. 160 (2010) 1392–1396.
[15] Q. Liu, Y. Wang, Y. Zhang, S. Xu, J. Wang, Effect of dopants on the adsorbing performance of polypyrrole/graphite electrodes for capacitive deionization process, Synth. Met. 162 (2012) 655–661.
[16] C.A. Marina Mastragostino, Francesca SoaviConducting polymers as electrode materials in supercapacitors, Solid State Ionics 148 (2002) 493–498.
[17] K.-S. Kim, S.-J. Park, Bridge effect of silver nanoparticles on electrochemical performance of graphite nanofiber/polyaniline for supercapacitor, Synth. Met. 162 (2012) 2107–2111.
[18] L. Li, K. Xia, L. Li, S. Shang, Q. Guo, G. Yan, Fabrication and characterization of free-standing polypyrrole/graphene oxide nanocomposite paper, J. Nanopart. Res. 14 (2012) 908–915.
[19] Y. Li, H. Peng, G. Li, K. Chen, Synthesis and electrochemical performance of sandwich-like polyaniline/graphene composite nanosheets, Eur. Polym. J. 48 (2012) 1406–1412.
[20] N.V. Blinova, J. Stejskal, M. Trchová, J. Prokeš, M. Omastová, Polyaniline and polypyrrole: A comparative study of the preparation, Eur. Polym. J. 43 (2007) 2331–2341.
[21] W.-X. Liu, N. Liu, H.-H. Song, X.-H. Chen, Properties of polyaniline/ordered mesoporous carbon composites as electrodes for supercapacitors, New Carbon Mater. 26 (2011) 217–223.
[22] Chen Yuanqiang, Zhang Yining Cheng Xiansu, Effects of electrochemical polymerization temperature on properties of PPy aluminum electrolytic capacitors, Electr. Compon. Mater. 29 (2010) 41–44.
[23] Y. Wu, Y. Wang, Y. Zhao, R. Wang, S. Xu, Preparation and application of DBS-PPy/CNTs composite as cathode material for capacitive deionization process, Shuichuli Jishu 39 (2013) 24–27.
[24] M.M. Ayad, W.A. Amer, M. Whdan, In situ polyaniline film formation using ferric chloride as an oxidant, J. Appl. Polym. Sci. 125 (2012) 2695–2700.
[25] Mi Hongyu, Zhang Xiaogang, Wu Quanfu, Effect of polymerization temperature on the electrochemical capacitance of polyaniline doped with acetic acid, Polym. Mater. Sci. Eng. 23 (2007) 128–131.
[26] B.-H. Park, J.-H. Choi, Improvement in the capacitance of a carbon electrode prepared using water-soluble polymer binder for a capacitive deionization application, Electrochim. Acta 55 (2010) 2888–2893.
[27] Y. Oren, Capacitive deionization (CDI) for desalination and water treatment—past, present and future (a review), Desalination 228 (2008) 10–29.
[28] D. Zhang, T. Yan, L. Shi, Z. Peng, X. Wen, J. Zhang, Enhanced capacitive deionization performance of graphene/carbon nanotube composites, J. Mater. Chem. 22 (2012) 14696–14704.
[29] H. An, Y. Wang, X. Wang, L. Zheng, X. Wang, L. Yi, L. Bai, X. Zhang, Polypyrrole/carbon aerogel composite materials for supercapacitor, J. Power Sources 195 (2010) 6964–6969.
[30] T.Q. Ma, Li, Research development of the conductive poly met materials—PAN. J. Chongqing Univ. 25 (2002) 124–127.
[31] L.-J. Bian, F. Luan, S.-S. Liu, X.-X. Liu, Self-doped polyaniline on functionalized carbon cloth as electroactive materials for supercapacitor, Electrochim. Acta 64 (2012) 17–22.